RESEARCH ARTICLE

Figures and figure supplements

Cells use molecular working memory to navigate in changing chemoattractant fields

Akhilesh Nandan *et al*

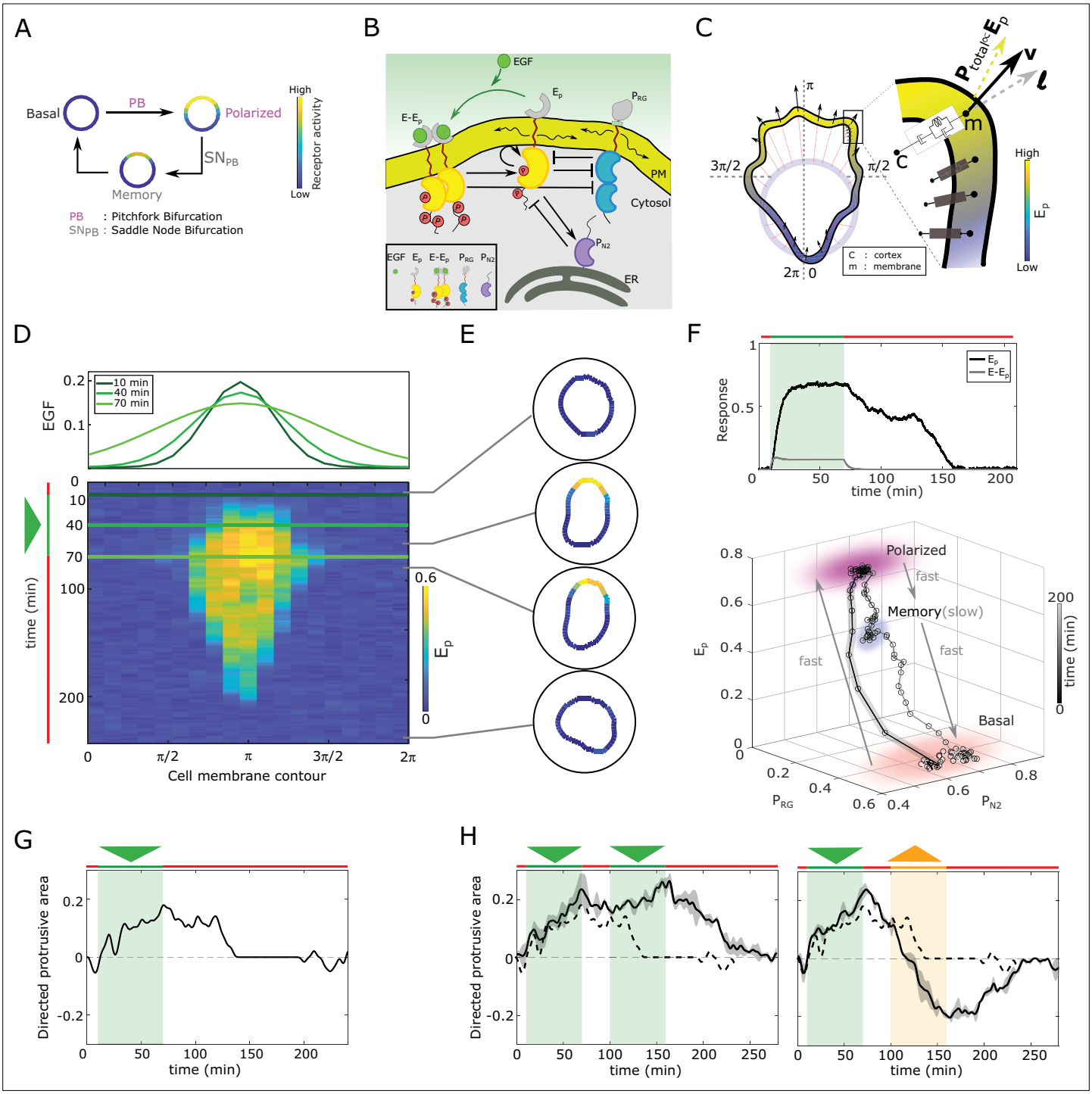

Figure 1. In silico manifestation of metastable polarized membrane signaling, as a mechanism for sensing changing spatial-temporal signals. **(A)** Dynamical mechanism: sub-critical pitchfork bifurcation (PB) determines stimulus-induced transition (arrow) between basal unpolarized and polarized receptor signaling state, whereas the associated saddle-node through which the PB is stabilized (SN_{PB}) gives rise to a "ghost" memory state upon signal removal for organization at criticality (before the SN_{PB}). See ***Figure 1—figure supplement 1A*** and Methods for detailed description of these transitions. **(B)** Scheme of the EGFR-PTP interaction network. Ligandless EGFR (E_p) interacts with PTPRG (P_{RG}) and PTPN2 (P_{N2}). Liganded EGFR ($E - E_p$) promotes autocatalysis of E_p. Causal links - solid black lines; curved arrow lines - diffusion, PM - plasma membrane, ER- endoplasmic reticulum. See also ***Figure 1—figure supplement 1B, C***, Signal-induced shape-changes during cell polarization. Arrows: local edge velocity direction. Zoom: Viscoelastic model of the cell - parallel connection of an elastic and a viscous element. $\mathbf{P_{total}}$: total pressure; v: local membrane velocity; l: viscoelastic state. Bold letters: vectors. Cell membrane contour: $[0, 2\pi]$. **(D)** Top: In silico evolution of spatial EGF distribution. Bottom: Kymograph of E_p for organization at criticality from reaction-diffusion simulations of the network in (**B**). Triangle - gradient duration. **(E)**, Corresponding exemplary

Figure 1 continued on next page

Figure 1 continued

cell shapes with color coded E_p, obtained with the model in (**C**). **(F)**, Top: Temporal profiles E_p (black) and $E - E_p$ (gray). Green shaded area: EGF gradient presence. Bottom: State-space trajectory of the system with denoted trapping state-space areas (colored) and respective time-scales. See also ***Figure 1—video 1***. Thick/thin line: signal presence/absence. (**G)**, Quantification of in silico cell morphological changes from the example in **(E)**. Triangle - gradient duration. (**H)**, Left: same as in (**G)**, only when stimulated with two consecutive dynamic gradients (triangles) from same direction. Second gradient within the memory phase of the first. See also ***Figure 1—figure supplement 1D***. Right: the second gradient (orange triangle) has opposite direction. See also ***Figure 1—figure supplement 1E***. Dashed line: curve from (**G)**. Mean±s.d. from n=3 is shown. Parameters: Methods. In (**D-H**), green(orange)/red lines: stimulus presence/absence.

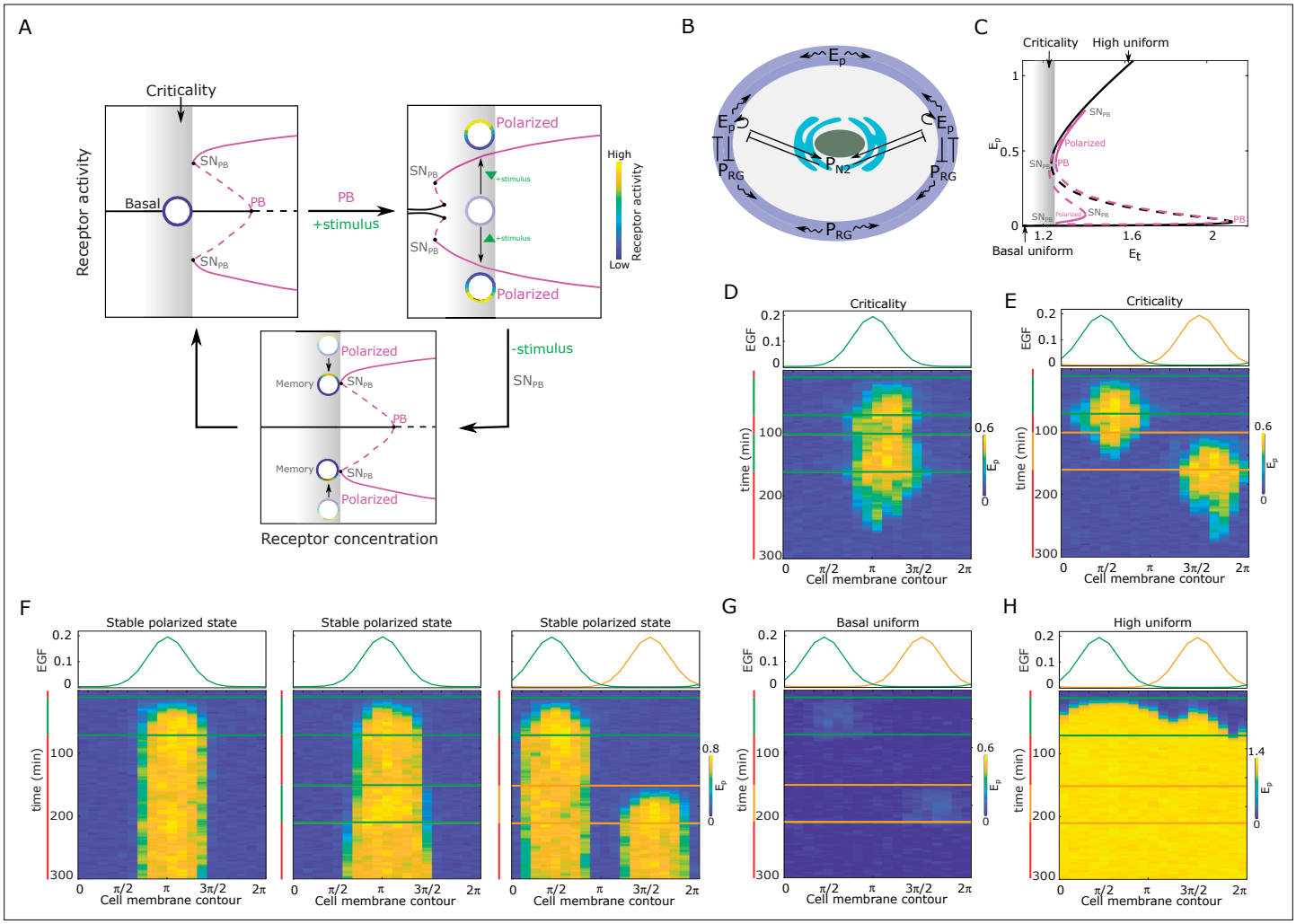

Figure 1—figure supplement 1. Features of receptor activity for different organization in parameter space. **(A)** Dynamical mechanism of signal-induced polarization and subsequent memory. Top, left: critical organization before sub-critical pitchfork bifurcation (PB, grey shaded area). SN_{PB}: saddle-node bifurcation through which PB is stabilized. Top, right: Stimulus induces unfolding of the PB. For the same organization (gray shaded area) the system is now in the stable polarized state (inhomogeneous steady state, IHSS). Bottom: After stimulus removal and disappearance of the SN_{PB}, the systems is transiently trapped in the "ghost" of this bifurcation, causing memory of the polarized state. Stable/unstable steady states (solid/dashed lines): basal (homogeneous, black) and polarized (inhomogeneous, magenta) receptor activity; stimulus induced transitions between states: arrow lines; circles: schematic representation of cell; color bar: receptor activity. **(B)** Spatial representation of the EGFR sensing network shown in ***Figure 1B***. E_p - phosphorylated EGFRR, P_{RG} - PTPRG; P_{N2} - PTPN2, solid lines: causal interactions, curved lines: diffusion. **(C)** Bifurcation diagram of the EGFR sensing network. Notations and line description as in A. E_t: total EGFR on the plasma membrane. Parameters in Methods. **(D)** Top: Position of two subsequent dynamic EGF gradients in the numerical simulation. Bottom: Representative in silico kymograph of EGFR phosphorylation (E_p) for organization of the system at criticality. Shape changes depicted in ***Figure 1H***, left. **(E)** Same as in (**D**), only when the second gradient (yellow) is from the opposite direction. Corresponding shape changes depicted in ***Figure 1H***, right. (**F**) Position of dynamic EGF signals(s) in the numerical simulation (top) and respective kymographs of EGFR activity changes (bottom) for organization of the system in the stable inhomogeneous state (magenta attractor in (**C**)). Left: Single dynamic gradient; Middle: a temporally disrupted gradient represented by two subsequent dynamic gradients from the same direction; Right: Second gradient (orange) from the opposite direction. **(G)** Same as in (**E**), only for organization in the homogeneous steady state representing symmetric basal EGFR phosphorylation (lower solid black line in **C**). **(H)** Same as in (**E**) only for organization in the homogeneous steady state representing uniform high EGFR phosphorylation (upper solid black line in **C**). For (**C-H**) parameters in Methods. Vertical green(orange)/red lines: stimulus presence/absence.

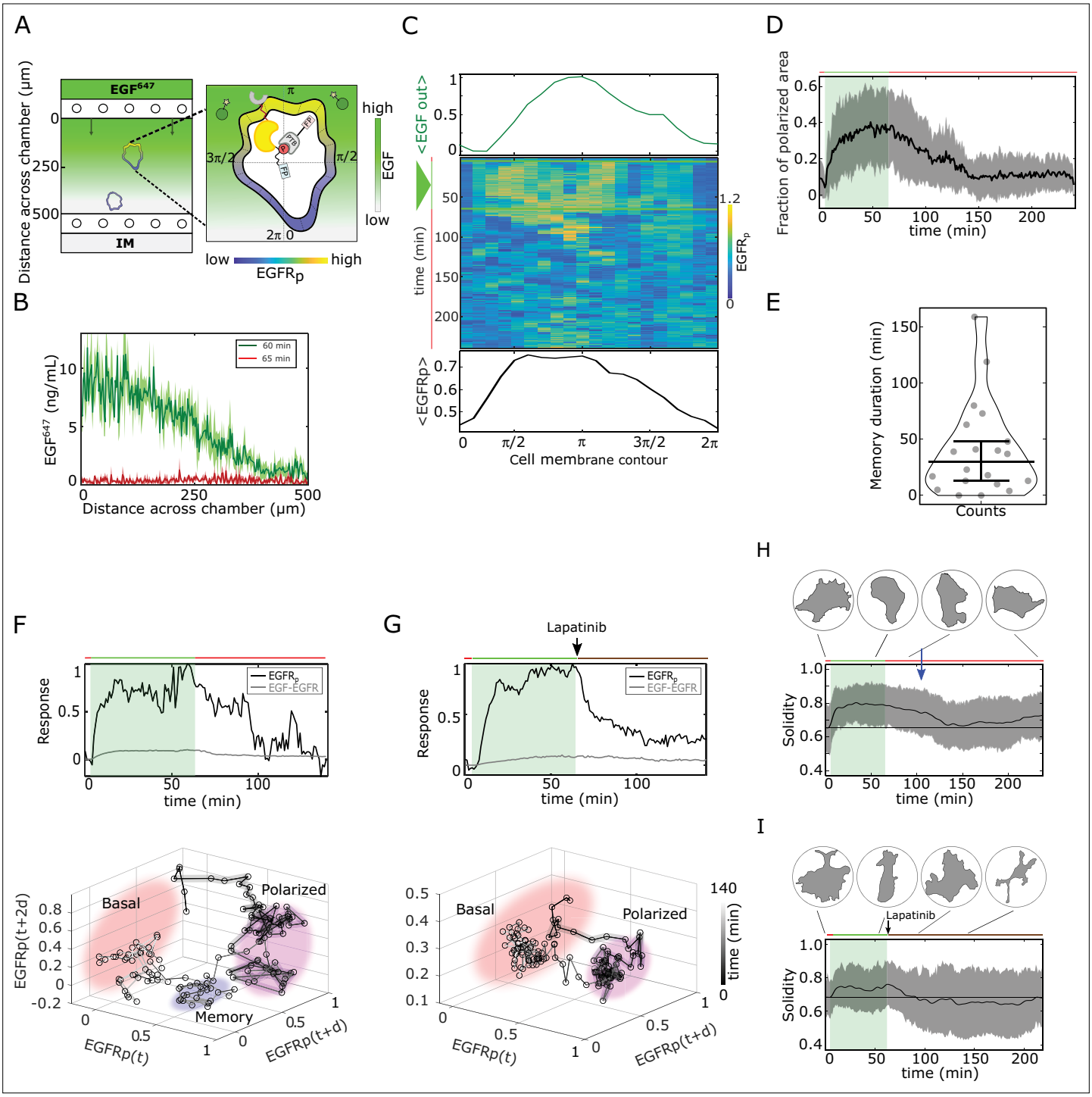

Figure 2. Molecular memory in polarized EGFR *mCitrine* phosphorylation resulting from dynamical state-space trapping is translated to memory in polarized cell shape. **(A)** Scheme of microfluidic EGF^{647}-gradient experiment; Zoom: single-cell measurables. Cell membrane contour $[0, 2\pi]$ (20 segments). PTB - phosphotyrosine binding domain, FP/star symbol - fluorescent protein, $EGFR_p$- phosphorylated EGFR *mCitrine*. Remaining symbols as in ***Figure 1B***. (**B**) Quantification of EGF^{647} gradient profile (at $60min$, green) and after gradient wash-out (at $65min$, red). Mean ± s.d., N=4. (**C**) Exemplary quantification of, Top: Spatial projection of EGF^{647} around the cell perimeter. Gaussian fit of the spatial projection is shown. Middle: single-cell $EGFR_p$ kymograph. Data was acquired at $1min$ intervals in live MCF7-EGFR *mCitrine* cells subjected for $60min$ to an EGF^{647} gradient. Other examples in ***Figure 2—figure supplement 1D***. Bottom: respective spatial projection of $EGFR_p$. Gaussian fit of the spatial projection is shown. Mean±s.d. from n=20 cells, N=7 experiments in ***Figure 2—figure supplement 1C***. (**D**) Average fraction of polarized plasma membrane area (mean±s.d.). Single cell profiles in ***Figure 2—figure supplement 1G***. (**E**) Quantification of memory duration in single cells (median±C.I.). In D and E, n=20, N=7. (F) Top: Exemplary temporal profiles of phosphorylated $EGFR^{mCitrine}$ (black) and $EGF^{647} - EGFR^{mCitrine}$ (gray) corresponding to (**C**). Bottom: Corresponding

Figure 2 continued on next page

Figure 2 continued

reconstructed state-space trajectory (***Figure 2—video 1***) with denoted trapping state-space areas (colored). Thick/thin line: signal presence/absence. d - embedding time delay. (**G**), Equivalent as in F, only in live MCF7-EGFR $mCitrine$ cell subjected to 1 h EGF^{647} gradient (green shading), and 3 h after wash-out with $1\,\mathrm{M}$ Lapatinib. Corresponding kymograph shown in ***Figure 2—figure supplement 2A***. Mean±s.d. temporal profile from n=9, N=2 in ***Figure 2—figure supplement 2B***. Bottom: Corresponding reconstructed state-space trajectory with state-space trapping (colored) (Methods, ***Figure 2—video 2***). H, Averaged single-cell morphological changes (solidity, mean±s.d. from n=20, N=7). Average identified memory duration (blue arrow): $40min$. Top insets: representative cell masks at distinct time points. I, Average solidity in MCF7-EGFR$mCitrine$ cells subjected to experimental conditions as in G. Mean±s.d. from n=9, N=2. Top insets: representative cell masks at distinct time points. In F-I, green shaded area: EGF^{647} gradient duration; green/red lines: stimulus presence/absence. Orange line: Lapatinib stimulation. See also ***Figure 2—figure supplements 1 and 2***.

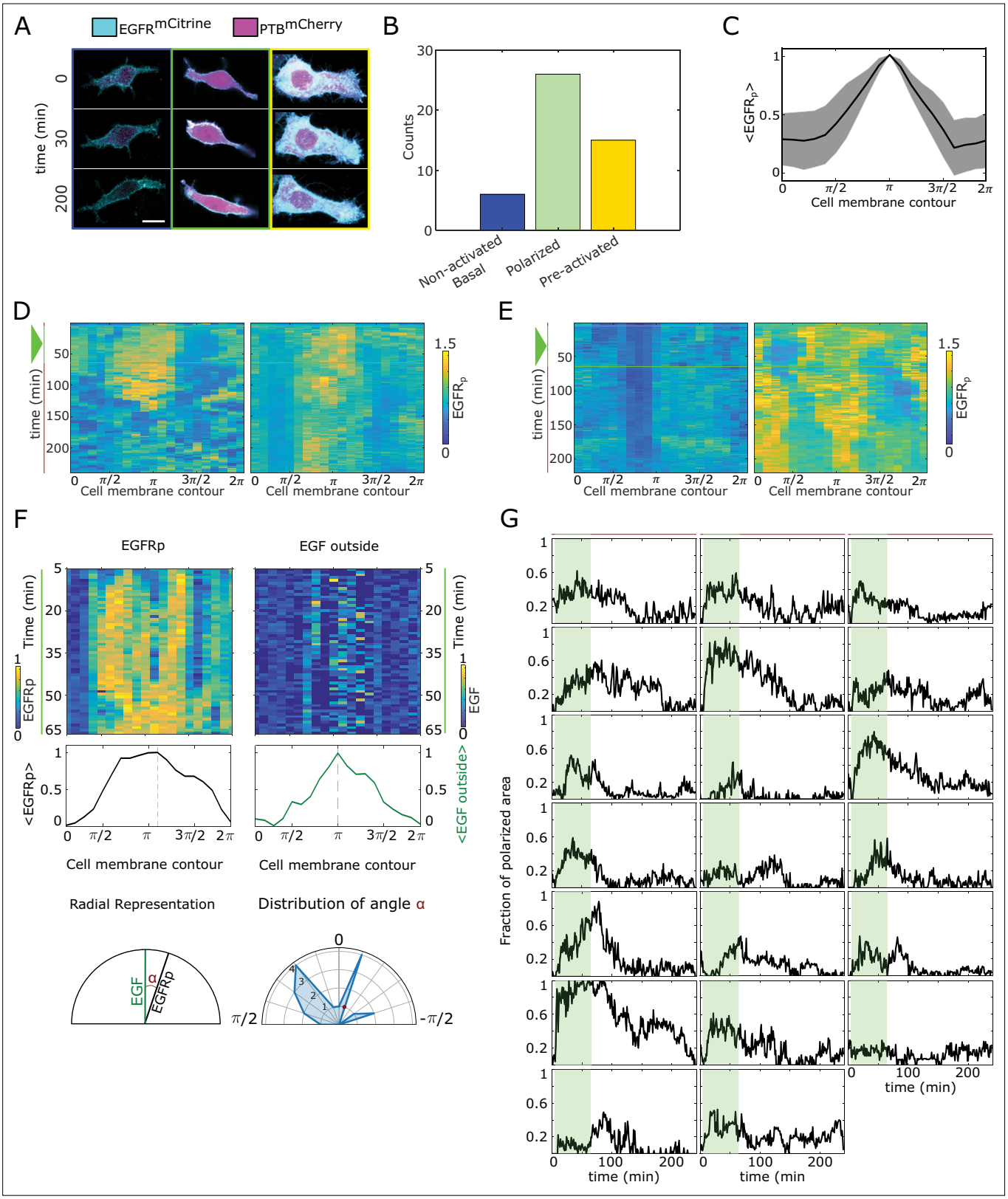

Figure 2—figure supplement 1. Quantification of EGFR$_{mCitrine}$ phosphorylation polarization. (**A**) Representative images / overlay of EGFR$_{mCitrine}$ (cyan) and PTB $_{mCherry}$ (magenta) prior to ($0min$), during ($30min$) and after ($200min$) MCF7-EGFR$_{mCitrine}$ cells were subjected to $60min$ EGF^{647} gradient. Columns: non-activated (blue), transiently polarized (green) and uniformly pre-activated (yellow). Scale bar: $15\mu m$. (**B**) Distribution of single-cell responses corresponding to A from $N = 7$ experiments. (**C**) Average profile of the spatial projection of the fraction of phosphorylated EGFR$_{mCitrine}$

Figure 2—figure supplement 1 continued on next page

Figure 2—figure supplement 1 continued

from single-cell kymographs. For each cell, temporal average per spatial bin is calculated, and the final spatial profile was estimated as an average of a moving window of 7 points. Peaks of the single-cell distributions were shifted to π before averaging. Mean±s.d. from n=20 cells, N=7 experiments is shown. (**D**) Additional exemplary single-cell kymographs depicting polarized EGFR $_{mCitrine}$ phosphorylation. Data acquisition and quantification as in ***Figure 2C***. Triangle: gradient duration. (**E**) Same as in D, only for non-activated (basal, left) and uniformly pre-acivated (right) EGFR$_{mCitrine}$ phosphorylation. Triangle: gradient duration. (**F**) Quantification of direction of polarization of EGFR$_{mCitrine}$ phosphorylation. Top: exemplary kymographs of $EGFR_p$ (left) and EGF^{647} outside the cells (right) during the gradient stimulation (60 min). Data corresponds to ***Figure 2C***. Middle: respective spatial projection of $EGFR_p$ and EGF^{647}. Average using a moving window of 7 bins is shown. Bottom: Schematic representation of identifying direction of polarization. Left: angle (α) between $EGFR_p$ and EGF^{647} is estimated as the angle between the maxima of the spatial projections (shown in middle plots). Right: distribution of α calculate from n=20 cells, N=7 experiments. G, Temporal profiles of the estimated fraction of polarized area for single cells. Green shaded area: EGF^{647} gradient duration. The mean ± s.d. shown in ***Figure 2D***.

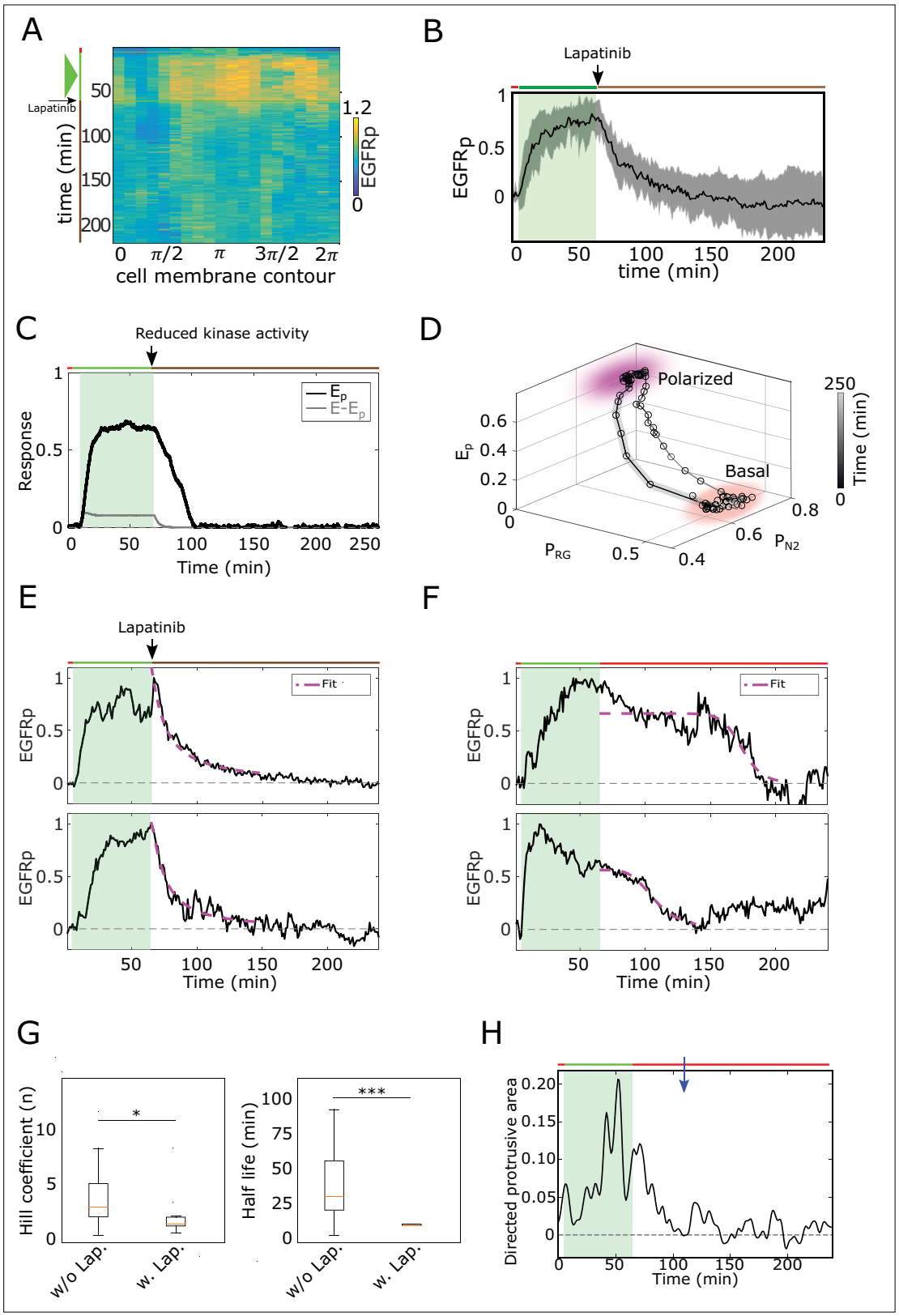

Figure 2—figure supplement 2. Memory in polarized $EGFR_p$ results from a dynamical "ghost". (**A**) Exemplary single-cell kymograph depicting phosphorylated EGFR$_{mCitrine}$ for data acquired at $1min$ intervals in live MCF7-EGFR $_{mCitrine}$ cell subjected for 1 h to EGF^{647} gradient, and 3 h duringr gradient wash-out with $1\,\mathrm{M}$ Lapatinib. (**B**) Average temporal profiles of plasma membrane EGFR$_{mCitrine}$ phosphorylation of live MCF7-EGFR$_{mCitrine}$ cells subjected for 1 h to EGF^{647} gradient, and 3 h during gradient was-out with $1\,\mathrm{M}$ Lapatinib. Related to ***Figure 2G***. Mean ± s.d. from n=9, N=2 is

Figure 2—figure supplement 2 continued on next page

Figure 2—figure supplement 2 continued

shown. Green shaded area: EGF^{647} gradient. (**C**) In silico temporal profiles of E_p (black) and $E - E_p$ (gray), when the kinase activity of the receptor is inhibited after gradient removal by decreasing the autocatalytic rate constant ($\alpha_2 = 0.25$). Green shaded area: EGF gradient presence. (**D**) State-space trajectory corresponding to the example in C, with denoted trapping state-space areas (colored). Thick/thin line: signal presence/absence. See also ***Figure 2—video 3***. (**E**) Exemplary profiles of $EGFR_p$ (black) and corresponding fit with an inverse sigmoid function after gradient removal (magenta) of MCF7-$EGFR_{mCitirine}$ cell subjected for 1 h to an EGF^{647} gradient, and 3 h wash-out with $1\,\mathrm{M}$ Lapatinib. (**F**), Same as in E, but for cells without Lapatinib treatment. (**G**) Left: Hill coefficient estimated from single-cell fits with inverse sigmoid function as in E, F. Right: Corresponding half-life estimates. n=23, N=5, (without Lapatinib) and n=12, N=5 (with Lapatinib). Error bars: median±95%C.I (**H**) Exemplary quantification of morphological changes using directed cell protrusion area for the cell shown in ***Figure 2C***. Estimated memory duration: $43min$ (blue arrow).

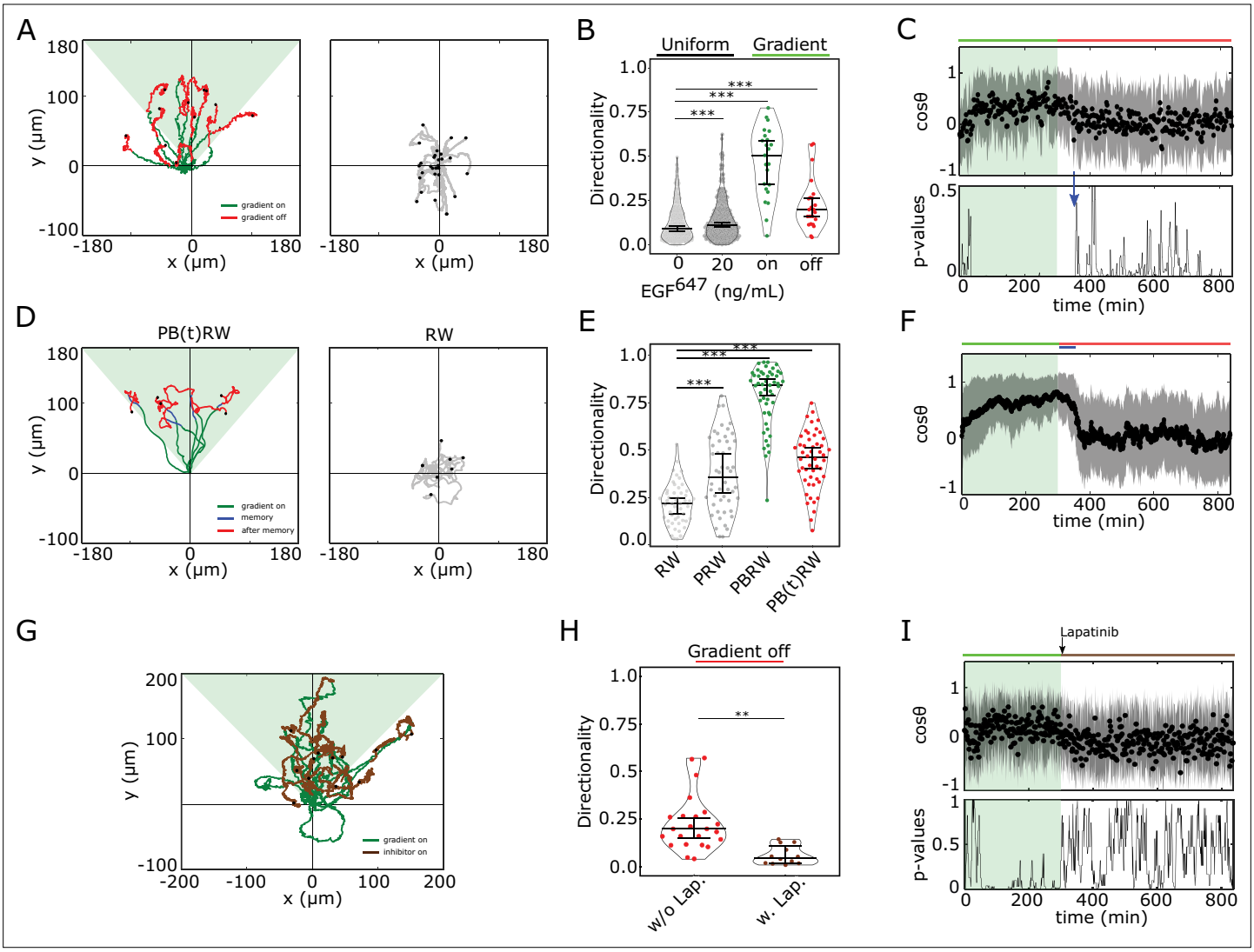

Figure 3. Cells display memory in directional migration towards recently encountered signals. **(A)**, Left: representative MCF10A single-cell trajectories. Green - 5 h during and red line - 9 h after dynamic EGF^{647} gradient (shaded). Exemplary cell in ***Figure 3—video 1***. Right: Same as in A, only 14 h in continuous EGF^{647} absence. Black dots: end of tracks. **(B)**, Directionality (displacement/distance) in MCF10A single-cell migration during 14 h absence (0 ng/ml; n=245, N=3) or uniform 20 ng/ml EGF^{647} stimulation (n=297, N=3); 5 h dynamic EGF^{647} gradient (green) and 9 h during wash-out (red; n=23, N=5). p-values: $***p\leq0.001$, two-sided Welch's t-test. Error bars: median±95%C.I. **(C)**, Top: Projection of the cells' relative displacement angles (mean±sd; n=23, N=5) during (green shaded) and after 5 h dynamic EGF^{647} gradient. Green/red lines: stimulus presence/absence. Bottom: Kolmogorov-Smirnov (KS) test p-values depicting end of memory in directional migration (blue arrow, $t = 350min$). KS-test estimated using 5 time points window. For **(A-C)**, data sets in ***Figure 3—figure supplements 1D and 2A***. **(D)**, Representative in silico single-cell trajectories. Left: PB(t)RW: Persistent biased random walk, bias is a function of time (green/blue trajectory part - bias on). Right: RW: random walk. **(E)**, Corresponding directionality estimates from n=50 realizations, data in ***Figure 3—figure supplement 2D***. PRW: persistent random walk. p-values: $***p\leq0.001$, two-sided Welch's t-test. Error bars: median±95%C.I. F, Same as in **(C)**, top, only from the synthetic PB(t)RW trajectories. **(G)**, MCF10A single-cell trajectories quantified 5 h during (green) and 9 h after (orange) dynamic EGF^{647} gradient (shading) wash-out with $3\,\mathrm{M}$ Lapatinib. n=12, N=5. See also ***Figure 3—video 2***. **H**, Directionality in single-cell MCF10A migration after gradient wash-out with (brown, n=12, N=5) and without Lapatinib (red, n=23, N=5). p-values: $**p\leq0.01$, KS-test. Error bars: median±95%C.I. I, Same as in **(C)**, only for the cells in G. See also ***Figure 3—figure supplement 2H***.

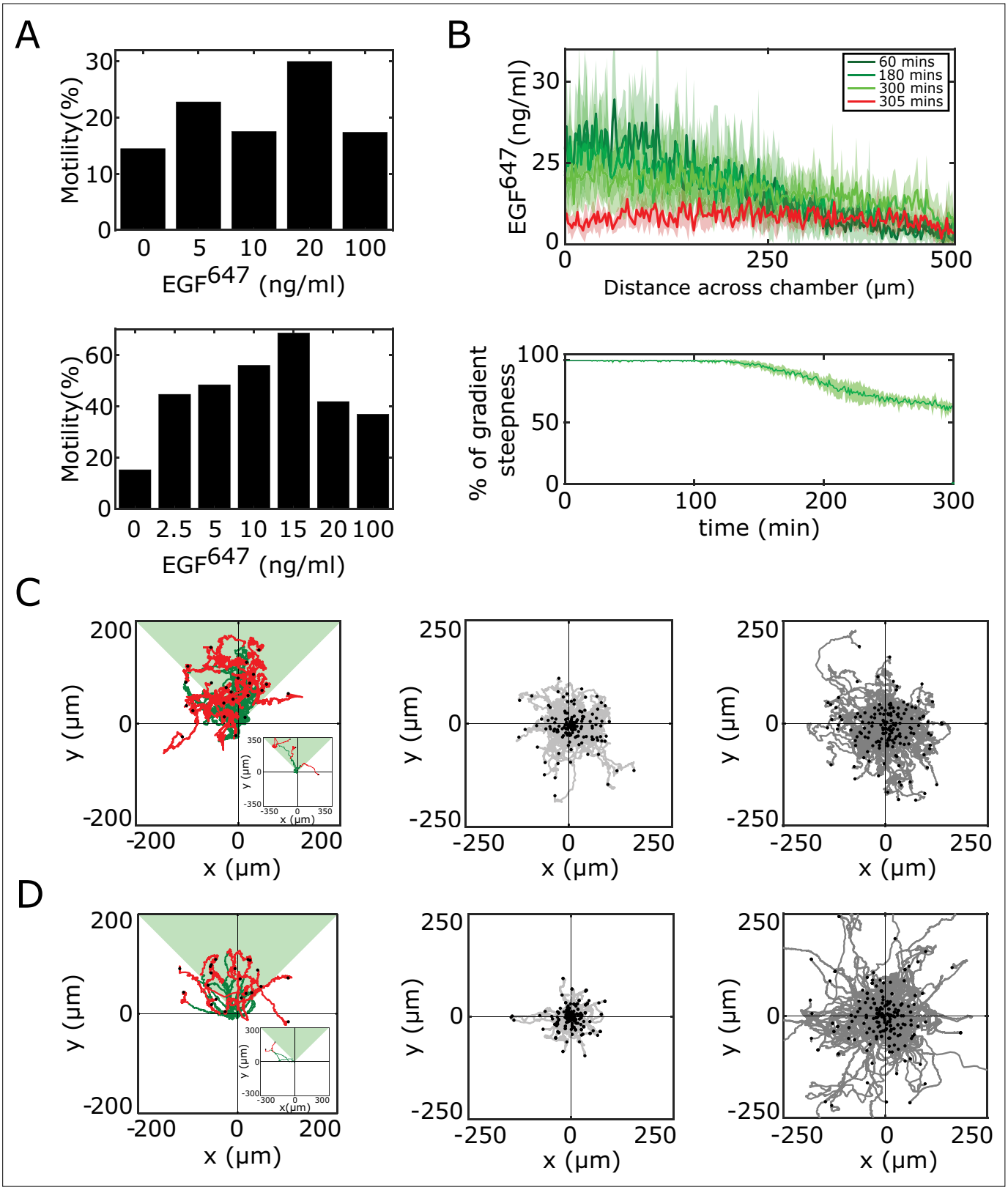

Figure 3—figure supplement 1. Characterization of MCF7-EGFR *mCitrine* and MCF10A single-cell migration. (**A**), Identification of optimal EGF^{647} dose range for single-cell gradient migration assay for MCF7-EGFR*mCitrine* (top) and MCF10A (bottom). Percentage of cell having motility greater than a displacement threshold ((Number of cell tracks with track length greater than threshold/Total number of cells)*100) is shown. (**B**), Top: Quantification of 5 h dynamic EGF^{647} gradient at distinct time-points. Bottom: Corresponding quantification of the temporal evolution of the gradient slope. Percentage

Figure 3—figure supplement 1 continued on next page

Figure 3—figure supplement 1 continued

of gradient steepness: $((EGF_{(0)}^{647} - EGF_{(L)}^{647})/EGF_{(0)}^{647}) * 100$ where L is the length across the chamber. Mean±s.d. from N=4 is shown. (**C**), Divergence plots depicting MCF7-EGFR$_{mCitrine}$ single-cell trajectories quantified, left: 5 h during (green) and for 9 h after (red) dynamic EGF^{647} gradient duration (n=26, N=7); middle: 14 h of 0 ng/ml EGF^{647} (subset of n=207 from n=426 is shown, N=2); and right: 14 h of uniform 20 ng/ml EGF^{647} stimulation (subset of n=200 from n=456 is shown, N=2). (**D**), Same as in (**C**), only for MCF10A cells. Left: n=23, N=5; middle: n=245, N=3; right: n=297, N=3. Related to ***Figure 3A–C***. Black dots: end of tracks.

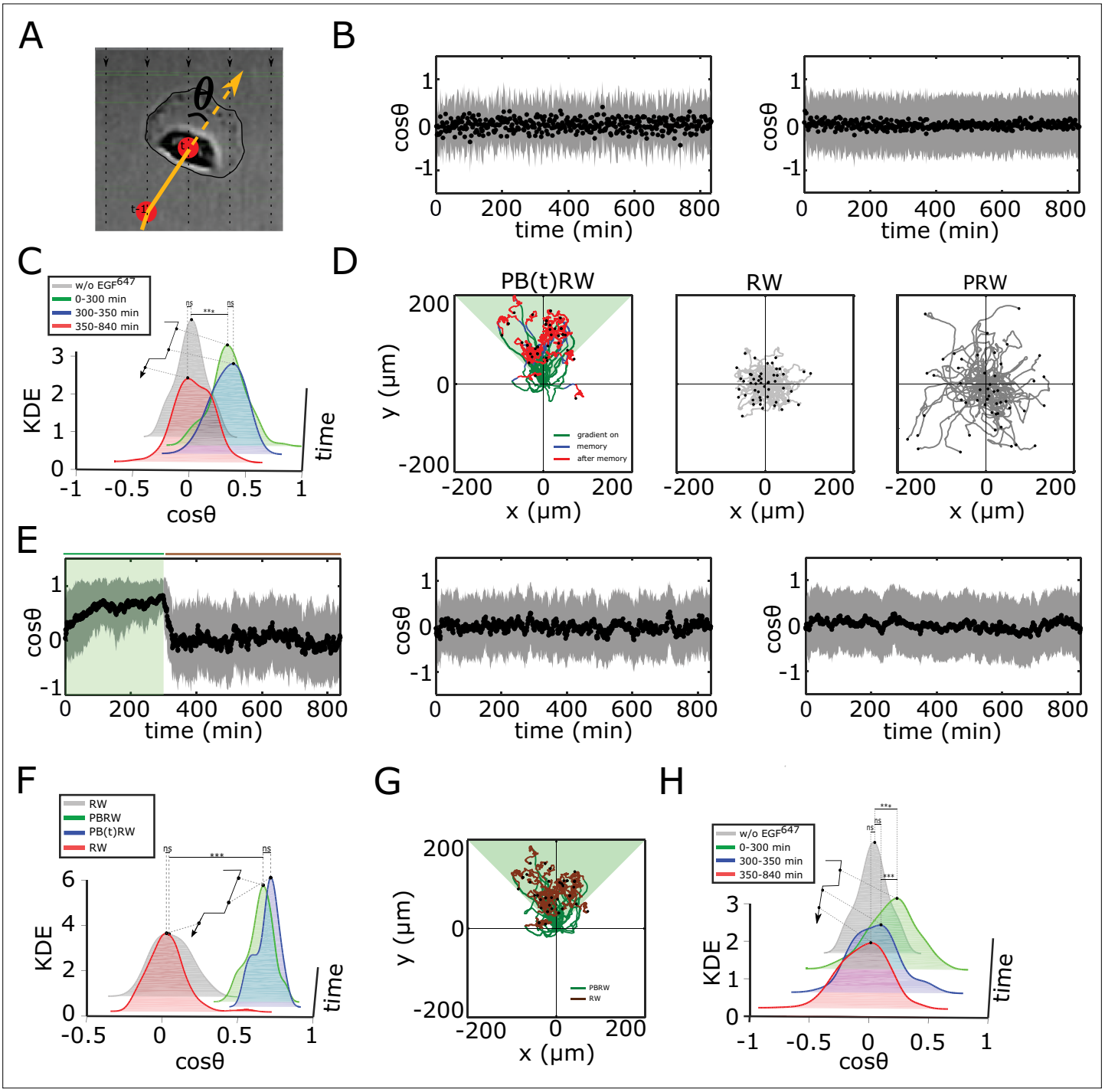

Figure 3—figure supplement 2. Characterization of single cell migration patterns. (**A**), Scheme of single-cell relative displacement angle estimation ($\cos\theta$). (**B**), Average $\cos\theta$ from single MCF10A cell trajectories (mean±sd), estimated over a $2min$ interval upon, left: 0 ng/ml EGF^{647} (n=245, N=3); right: 20 ng/ml uniform EGF^{647} stimulation (n=297, N=3). Related to ***Figure 3A–C***. (**C**), Kernel density estimates (KDE) of the distributions in (**B**) and ***Figure 3C*** top, in continuous EGF^{647} absence (gray), during 5 h dynamic EGF^{647} gradient (green), after gradient wash-out: $t \in [300min, 350min]$ (blue) and $t \in [350min, 840min]$ (red). p-values: $***$, p≤0.001, ns: not significant, KS-test. (D), Synthetic single-cell trajectories (***Equation 7***, Methods). Left: Persistent biased random walk PB(t)RW; middle: random walk (RW); right: Persistent random walk (PRW). Parameters: for PB(t)RW, $\tau = 38.143$, $b(t) = 0.134$, $D = 2.207$ for $t \in [0min, 350min]$ (green,blue), $\tau = 11.105$, $b(t) = 0$, $D = 0.425$ for $t \in [350min, 840min]$ (red); for RW, $\tau = 11.105$, $b(t) = 0$, $D = 0.425$; for PRW, $\tau = 38.143$ and $D = 2.207$. (**E**), Same as in (**B**)., only from the synthetic trajectories. Left: PB(t)RW with $\tau = 38.143$, $D = 2.207$, $b(t) = 0.134$ for $t \in [0min, 300min]$ (green shading), $\tau = 11.105$, $D = 0.425$, $b(t) = 0$ for $t \in [300min, 840min]$, middle: RW; right: PRW. (**F**), Same as in (**C**), only from the synthetic trajectories. p-values: $***$, p≤0.001, ns: not significant, KS-test. (**G**), Synthetic single cell trajectories

Figure 3—figure supplement 2 continued on next page

Figure 3—figure supplement 2 continued

generated when PBRW is considered only in the time frame during gradient duration to mimic the experimental data in ***Figure 3G***. Parameters as in (E, left). (**H**), Same as in (C), only for MCF10A cells stimulated for 5 h with EGF^{647} gradient and 9 h after wash-out with $3\,\mathrm{M}$ Lapatinib. Related to ***Figure 3I***. p-values: $***$, $p \leq 0.001$, ns: not significant, KS-test.

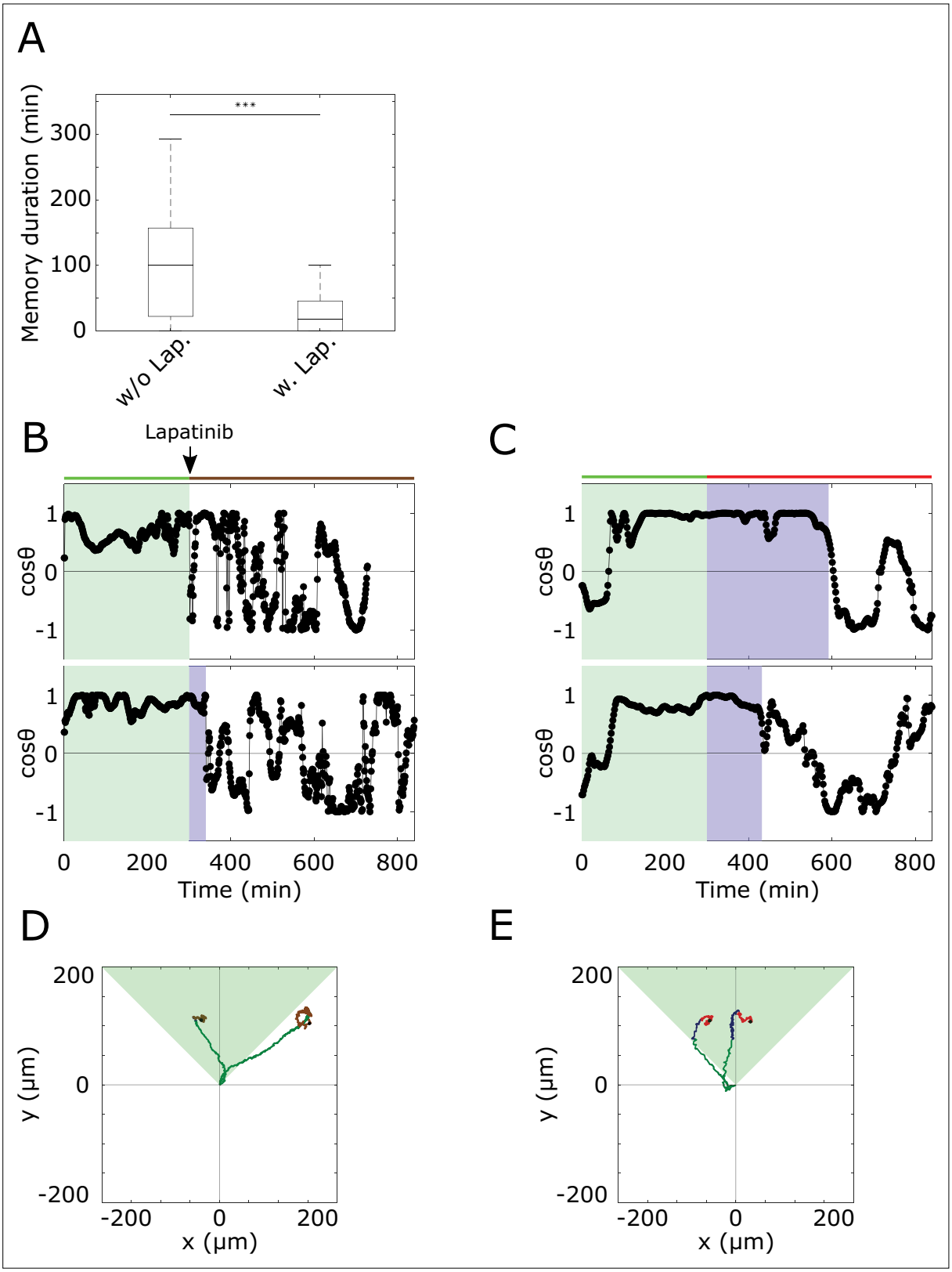

Figure 3—figure supplement 3. Quantifying duration of memory in directional migration from single-cell $\cos\theta$ profiles. (**A**), Duration of memory in directional migration of MCF10A cells treated with a 5 h dynamic EGF^{647} gradient (n=23, N=5; single cell tracks in ***Figure 3—figure supplement 1D***), and MCF10A cells treated with a 5 h dynamic EGF^{647} gradient, followed by 9 h 3μ M Lapatinib during gradient wash-out (n=12, N=5, single cell tracks in ***Figure 3G***). p-values: $***$ p$\leq$0.001, two-sided Welch's t-test. Error bars: median±95%C.I. Values estimated from single-cell $\cos\theta$ plots. (**B**), Exemplary

Figure 3—figure supplement 3 continued on next page

Figure 3—figure supplement 3 continued

$\cos\theta$ plots estimated from MCF10A cell motility trajectories. Cells were treated with a 5 h dynamic EGF^{647} gradient, followed by 9 h 3μ M Lapatinib during gradient wash-out. Green shaded area denotes EGF^{647} gradient interval, blue shaded area - time interval of identified memory in directional migration (Methods). (**C**), Same as in (**B**), only without Lapatinib treatment. (**D**), Divergence plots of the cells shown in (B). Green part of the tracks denotes migration during gradient, blue - migration during identified memory phase after gradient removal, brown - random migration after gradient removal. Green shaded triangle: gradient direction. Black dots: end of tracks. (**E**), Divergence plots of the cells in (**C**). Color coding as in (**D**). Red: random migration after gradient wash-out.

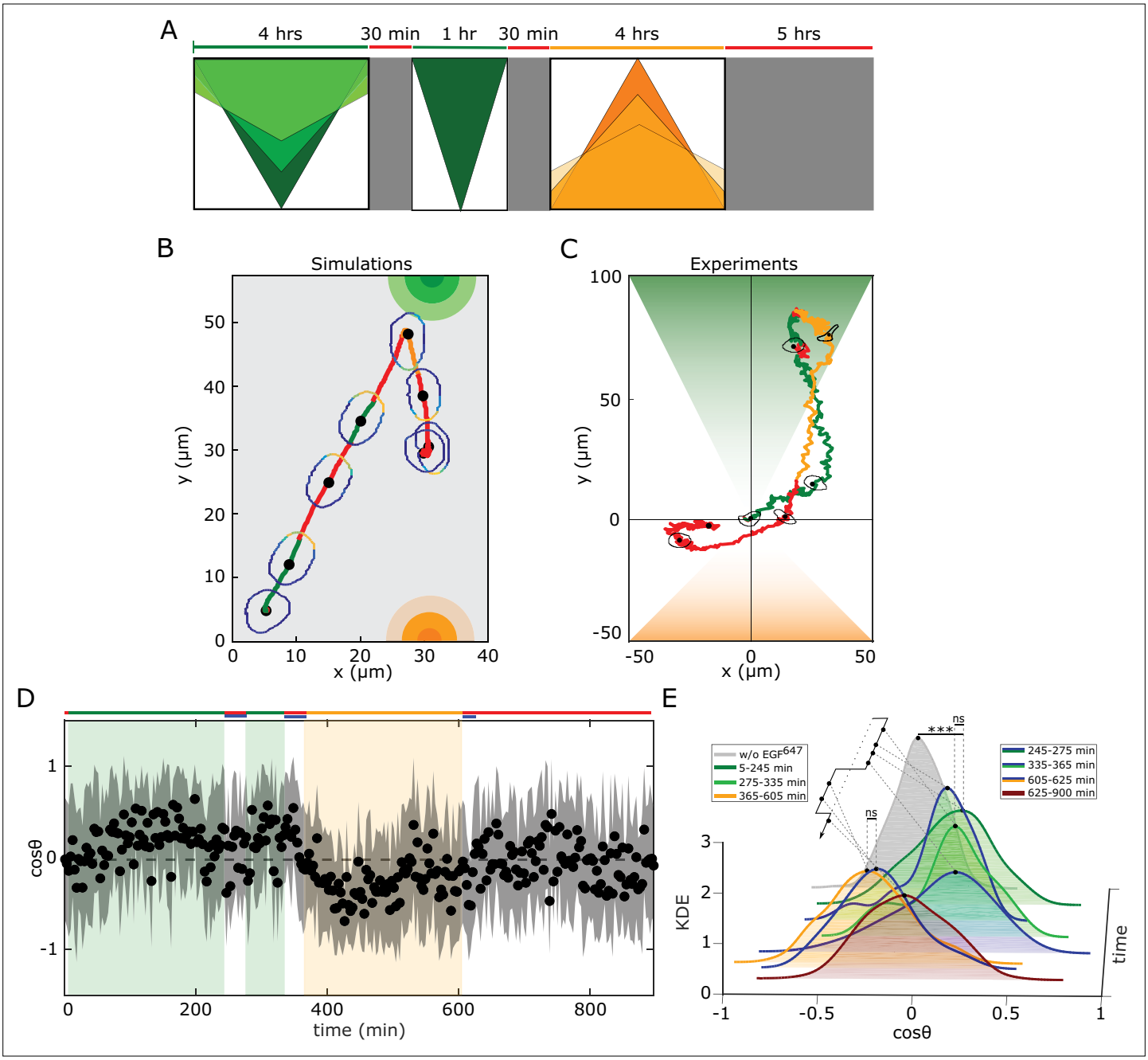

Figure 4. Working memory enables history-dependent single-cell migration in changing chemoattractant field. **(A)**, Scheme of dynamic spatial-temporal growth factor field implemented in the simulations and experiments. Green(orange)/red: gradient presence/absence. (**B**), In silico cellular response to the sequence of gradients as depicted in A, showing changes in EGFR activity, cellular morphology and respective motility trajectory over time. Trajectory color coding corresponding to that in (**A**), cell contour color coding with respective E_p values as in ***Figure 1E***. Cell size is magnified for better visibility. See also ***Figure 4—figure supplement 1A***, ***Figure 4—video 1***. **(C)**, Representative MCF10A single-cell trajectory and cellular morphologies at distinct time-points, when subjected to dynamic EGF^{647} gradient field as in A (gradient quantification in ***Figure 4—figure supplement 1E***). Trajectory color coding corresponding to that in A. See also ***Figure 4—video 4***. Full data set in ***Figure 4—figure supplement 1F***. **(D)**, Projection of cells' relative displacement angles ($\cos\theta$) depicting their orientation towards the respective localized signals. Mean±s.d. from n=12, N=5 is shown. E, Corresponding kernel density estimates (intervals and color coding in legend). p-values: $***$, $p \leq 0.001$, ns: not significant, KS-test.

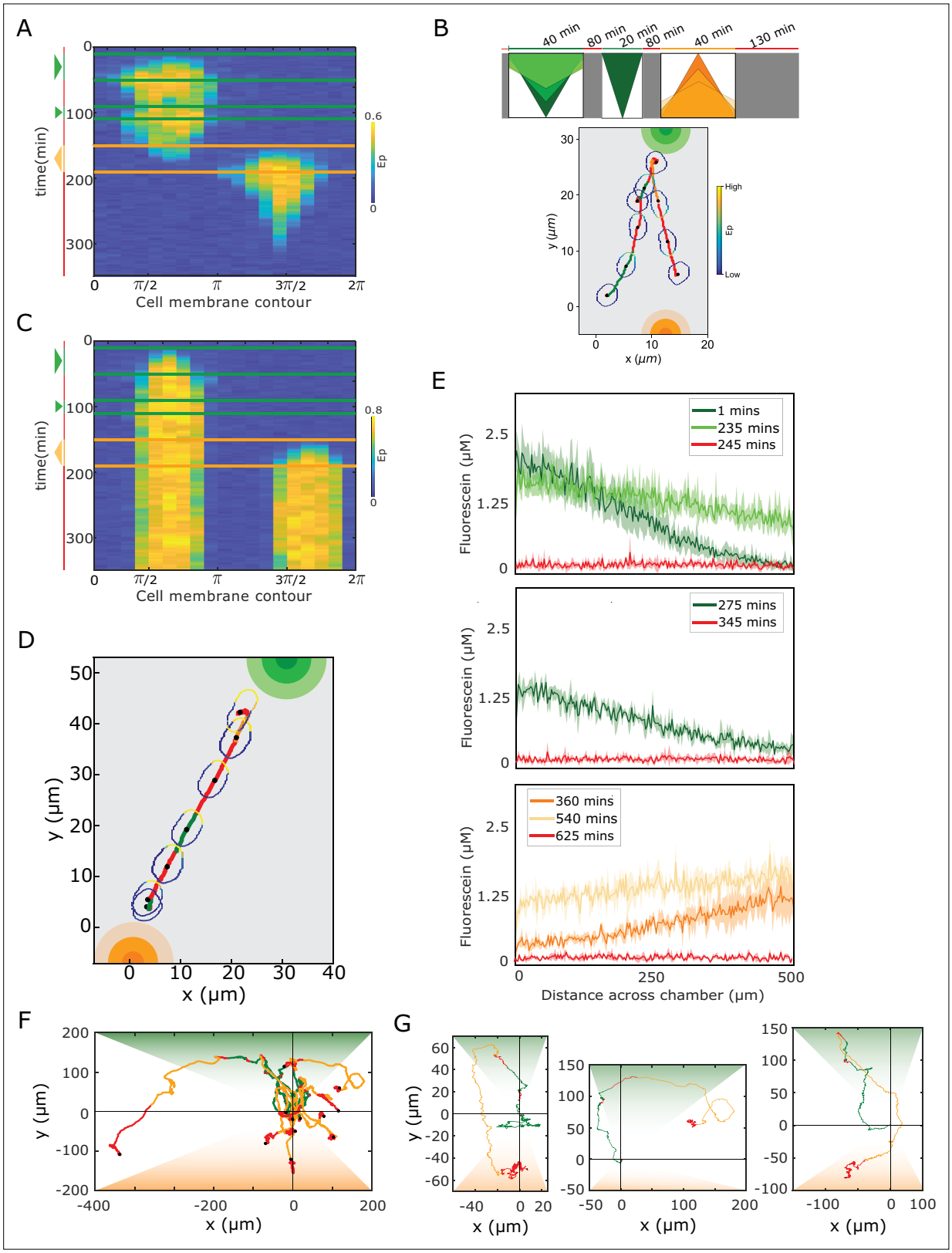

Figure 4—figure supplement 1. Single-cell navigation in changing growth factor fields. **(A)**, In silico obtained E_p kymograph corresponding to ***Figure 4B***. Parameters in Methods. **(B)**, In silico cellular response to a sequence of gradients as depicted on top, showing changes in EGFR activity, cellular morphology and respective motility trajectory over time. Trajectory color coding corresponding to scheme on top, cell contour color coding with respective E_p values as in ***Figure 1E***. Cell size is magnified for better visibility. See also ***Figure 4—video 2***. **(C)**, E_p kymograph obtained for organization

Figure 4—figure supplement 1 continued on next page

Figure 4—figure supplement 1 continued

in the stable polarized state, when a cell is subjected to the gradient filed in ***Figure 4A***. **(D)**, Corresponding changes in cellular morphology and respective motility trajectory over time. Trajectory and E_p color coding as in **B**. Cell size is magnified for better visibility. See also ***Figure 4—video 3***. **(E)**, Quantification of a 15 h dynamic fluorescin at distinct time-points. Mean±s.d. from N=3 is shown. **(F)**, Divergence plots depicting MCF10A single-cell trajectories quantified during migration in dynamic EGF^{647} gradient filed shown in (**E**). n=12, N=5. Trajectory color-coding corresponding to the scheme in ***Figure 4A***. **G**, Zoomed exemplary single cell trajectories from **F**.

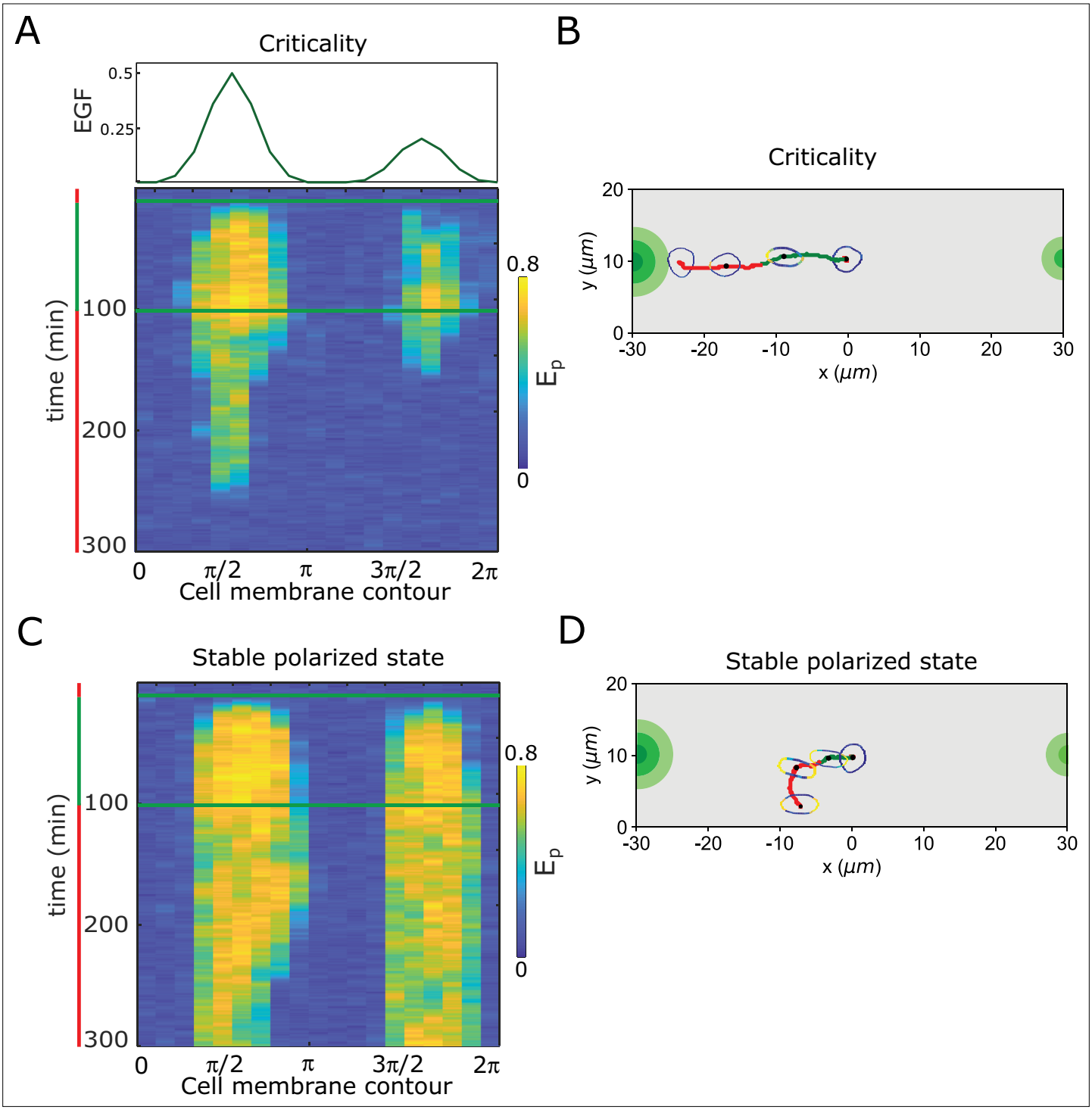

Figure 4—figure supplement 2. Resolving simultaneous signals with opposed localisation is optimal at criticality. **(A)**, Top: Position of two simultaneous EGF gradients with different amplitudes in the numerical simulation. Bottom: Representative in silico kymograph of EGFR phosphorylation (E_p) for organization of the system at criticality. **(B)**, Corresponding changes in cellular morphology and motility trajectory over time. Trajectory and E_p color coding as in **(A)**. Cell size is magnified for better visibility. See also ***Figure 4—video 5***. **(C)**, Same as in **(A)**, only for organization in the stable polarized state. **(D)**, Same as in **(B)**, only for organization in the stable polarized state (corresponding to C). See also ***Figure 4—video 6***.